(25 g)[27] in methylene chloride for 18 h. The mixture was filtered and evaporated. The residue was triturated with pentane, filtration and evaporation of which gave 1.0 g (28%) of product as a white solid. ^{13}C NMR ($CDCl_3$) 217.4, 44.5, 42.1, 41.7 (t, J_{CD} = 22 Hz), 27.7, 24.4, 23.0 ppm. ^1H NMR analysis using $Eu(fod)_3$ as a shift reagent showed the product to be ca. 90% deuterated at C_1 and 15% deuterated at C_3.

Acknowledgment. This work was supported by the National Science Foundation (CHE-8211125). We thank James Puckace for assistance with some of the spectra.

Registry No. 1, 51823-56-4; **1**-*exo*-3-*d*, 92720-86-0; **1**-*endo*-3-*d*, 92720-87-1; **1**-3,3-d_2, 92720-88-2; **2**, 51804-52-5; **2**-3-*d*, 92720-89-3; **2**-3,3-d_2, 92720-90-6; **2**-1-*d*, 92720-91-7; **3**, 51804-49-0; **3**-2,2,5,5-d_4, 91158-20-2; **4**, 25807-60-7; 4-d_6, 79663-74-4; bicyclo[2.2.1]heptan-2-one-*exo*-3-*d*, 18139-04-3; bicyclo[2.2.1]heptan-2-one-*endo*-3-*d*, 18139-05-4; bicyclo[2.2.2]octan-2-one-3-*d*, 92720-92-8; bicyclo[2.2.2]octan-2-one-3,3-d_2, 92720-93-9; bicyclo[2.2.2]octan-2-one-1-*d*, 92720-94-0; 2-cyclohexen-1-one-6,6-d_2, 83350-38-3; 2-((trimethylsilyl)oxy)-1,3-cyclohexadiene-1-*d*, 92720-95-1; D_2, 7782-39-0; 2-cyclohexen-1-one, 930-68-7; chlorotrimethylsilane, 75-77-4; phenyl vinyl sulfone, 5535-48-8.

Nuclear Magnetic Resonance Studies of Metalloporphyrin π-Cation Radicals as Models for Compound I of Peroxidases

Isao Morishima,* Yasuhiko Takamuki, and Yoshitsugu Shiro

Contribution from the Division of Molecular Engineering, Graduate School of Engineering, Kyoto University, Kyoto 606, Japan. *Received April 20, 1984*

Abstract: Hyperfine-shifted proton and deuterium NMR spectral studies are reported for ruthenium(II) and cobalt(III) octaethylporphyrin π-cation radicals, $[OEP{\cdot}Ru^{II}{\cdot}CO]^+{\cdot}Br^-$ (**1**), $[OEP{\cdot}Ru^{II}{\cdot}CO]^+{\cdot}ClO_4^-$ (**2**), $[OEP{\cdot}Co^{III}]^{2+}{\cdot}2Br^-$ (**3**), and $[OEP{\cdot}CO^{III}]^{2+}{\cdot}2ClO_4^-$ (**4**) and their meso-deuterated analogues. The meso proton (or deuterium) resonances were not seriously broadened for these radicals and exhibited upfield or downfield shifts depending on the counterions and the central metal. Non-Curie law behaviors for the meso proton shifts were interpreted in terms of a thermal equilibrium between $^2A_{1u}$ and $^2A_{2u}$ π-radical states which induce quite different electron spin distribution at the meso position. This thermal equilibrium was also confirmed by the variable-temperature UV spectral measurements. The thermodynamic parameters for this equilibrium were estimated and show that $^2A_{1u}$ and $^2A_{2u}$ states are energetically close and these two states are substantially mixed at room temperature. The downfield hyperfine shift of the meso proton for **2** was interpreted as arising from the π-cation radical in the predominant $^2A_{1u}$ state, and the substantial upfield shift for **1** was explained as due to mixing of the $^2A_{2u}$ state to the $^2A_{1u}$ state. These assignments are in disagreement with the well-documented ones based on the UV-vis spectral studies. The effect of the axial ligand, imidazole, on the NMR spectra of **1** was also studied to mimic the electronic state of compounds I of peroxidases.

Peroxidases and catalase (CAT) are hemoprotein enzymes which catalyze a wide variety of organic or inorganic compounds by hydrogen or alkyl peroxides.[1,2] These enzymes react with peroxide to produce an oxidized enzyme intermediate referred to as compound I, which possesses two oxidizing equivalents above the resting ferric state.[3-5] Compound I has been assigned to a ferryl porphyrin π-cation radical in which one oxidizing equivalent is stored in the form of a tetravalent iron stabilized by oxygen ($Fe^{IV}{=}O$) and the second equivalent resides in a porphyrin π-cation.[6-13] The porphyrin π-cation radical species has also been implicated in the chlorophyll photochemical reaction for the primary products generated by the photooxidation of the chlorins in the photosystems I and II[14] and, possibly, in the intermediate of the cytochrome P-450 reaction cycle.[15,16]

With relevance to these biological implications, the porphyrin π-cation radical has been subjected to a great deal of physicochemical study in recent years.[6] Mauzerall first reported generation of a stable porphyrin π-cation radical of magnesium(II) octaethylporphyrin by chemical oxidation.[17] Dolphin and his co-workers were able to oxdize several synthetic metalloporphyrins to a stable π-cation radical state.[6] Depending on the particular combination of solvents, porphyrins, central metals, and counterions, they found two types ($^2A_{1u}$ and $^2A_{2u}$) of porphyrin π-cation radicals having characteristic UV-vis spectra.[6a] ESR spectra and molecular orbital calculations suggest that the highest filled π-orbitals, a_{1u} or a_{2u}, of porphyrin are comparable in energy and

(1) Hewson, W. D.; Hager, L. P. "The Porphyrins"; Dolphin, D., Ed.; Academic Press: New York, 1978; Vol. 7, pp 295-332.
(2) Dunford, H. B.; Stillman, J. S. *Coord. Chem. Rev.* **1976**, *19*, 187-251.
(3) Blumberg, W. E.; Peisach, J.; Wittenberg, B. A.; Wittenberg, J. B. *J. Biol. Chem.* **1968**, *243*, 1854-1862.
(4) Brill, A. S.; Williams, R. J. P. *Biochem. J.* **1961**, *78*, 253-262.
(5) Palcic, M. M.; Rutter, R.; Araiso, T.; Hager, L. P.; Dunford, H. B. *Biochem. Biophys. Res. Comm.* **1980**, *94*, 1123-1127.
(6) (a) Dolphin, D.; Forman, A.; Borg, D. C.; Fajer, J.; Felton, R. H. *Proc. Natl. Acad. Sci. U.S.A.* **1971**, *68*, 614-618. (b) Dolphin, D.; Muljiani, Z.;Rousseau, K.; Borg, D. C.; Fajer, J.; Felton, R. H. *Ann. N.Y. Acad. Sci.* **1973**, *206*, 177-200. (c) Fajer, J.; Borg, D. C.; Forman, A.; Felton, R. H.; Vegh, L.; Dolphin, D. *Ibid.* **1973**, *206*, 349-364. (d) Felton, R. H.; Owen, G. S.; Dolphin, D.; Forman, A.; Borg, D. C.; Fajer, J. *Ibid.* **1973**, *206*, 504-515. (e) Fajer, J.; Borg, D. C.; Forman, A.; Adler, A. D.; Varadi, V. *J. Am. Chem. Soc.* **1974**, *96*, 1238-1239. (f) Felton, R. H. "The Porphyrins"; Dolphin, D., Ed.; Academic Press: New York, 1978; Vol. 5, pp 53-125. (g) Fajer, J.; Davis, M. S. "The Porphyrins"; Academic Press: New York, 1979; Vol. 4, pp 197-256. (h) Fujita, I.; Hanson, L. K.; Walker, F. Ann; Fajer, J. *J. Am. Chem. Soc.* **1983**, *105*, 3296-3300.
(7) (a) Loew, G. H.; Kert, C. J.; Hjelmeland, L. M.; Kircher, R. F. *J. Am. Chem. Soc.* **1977**, *99*, 3534-3535. (b) Loew, G. H.; Herman, Z. S. *Ibid.* **1980**, *102*, 6173-6174.
(8) Schulz, C. E.; Devaney, P. W.; Winkler, J.; Debrunner, P. G.; Doan, N.; Chiang, R.; Rutter, R.; Hager, L. P.; *FEBS Lett.* **1979**, *103*, 102-105.
(9) Chin, D. H.; Balch, A. L.; La Mar, G. N. *J. Am. Chem. Soc.* **1980**, *102*, 1446-1448.
(10) Hager, L. P.; Doubek, D. L.; Silverstein, R. M.; Hargis, J. H.; Martin, J. C. *J. Am. Chem. Soc.* **1972**, *94*, 4364-4366.
(11) (a) La Mar, G. N.; de Ropp, J. S. *J. Am. Chem. Soc.* **1980**, *102*, 395-397. (b) La Mar, G. N.; deRopp, J. S.; Smith, K. M.; Langry, K. C. *J. Biol. Chem.* **1981**, *256*, 237-243.
(12) Roberts, J. E.; Hoffman, B. M.; Rutter, R.; Hager, L. P. *J. Biol. Chem.* **1981**, *256*, 2118-2121; *J. Am. Chem. Soc.* **1981**, *103*, 7654-7656.
(13) Hanson, L. K.; Chang, C. K.; Davis, M. S.; Fajer. J. *J. Am. Chem. Soc.* **1981**, *103*, 663-670.
(14) (a) Barrett, J. *Nature (London)* **1967**, *215*, 733. (b) Goedheer, J. C. *Photochem. Photobiol.* **1967**, *6*, 521.
(15) Chang, C. K.; Dolphin, D. "Bioorganic Chemistry"; Van Tamelen, E. E., Ed., Academic Press: New York, 1978; Vol. 4, pp 37-80.
(16) Groves, J. T.; Kruper, W. J.; Nemo, T. E.; Myers, R. S. *J. Mol. Catal.* **1980**, *7*, 167-177.
(17) Fuhrhop, J.-H.; Mauzerall, D. *J. Am. Chem. Soc.* **1968**, *90*, 3875-3876.

0002-7863/84/1506-7666$01.50/0

that oxidation removes an electron from either one of them, depending on the conditions.[18,19] The remarkable difference of these two types of porphyrin π-cation radicals are the electron spin distribution on the porphyrin ring; for the $^2A_{2u}$ radical, large spin density is placed at the meso carbons and the pyrrole nitrogens, while the $^2A_{1u}$ radicals experience small spin density at the meso positions.[18]

On the basis of these model studies with the use of, in particular, the absorption and ESR spectra, it has been widely believed that horseradish peroxidase (HRP) compound I contains a porphyrin π-cation radical having an unpaired electron in the a_{2u} orbital.[6a] In fact, the recent analysis of the ENDOR spectrum of HRP compound I agrees qualitatively with the model of an $^2A_{2u}$ porphyrin cation radical, in which the hyperfine coupling of the radical with the pyrrole nitrogens was observed.[12] On the other hand, a similarity of the absorption spectra has also suggested that CAT compound I radical has an unpaired electron in the a_{1u} orbital.[6a] A CAT compound I type spectrum also has been reported for chloroperoxidase (CPO) compound I.[5] However, Rutter and his co-workers[20] have recently reported that ESR and Mössbauer properties of the compound I prepared from mesoheme-substituted HRP are quite similar, if not identical, to those of native HRP compound I, although the absorption spectrum is characteristic of $^2A_{1u}$ porphyrin π-cation radical[21] and different from that of the native HRP compound I. These findings allow one to expect that the UV–vis absorption spectra may not serve as a diagnosis to determine the electronic ground state of the porphyrin π-cation radical, and further that CAT and CPO compounds I may be in the $^2A_{2u}$ rather than the $^2A_{1u}$ porphyrin π-cation radical state.

We have previously reported in a preliminary communication[22] that the π-cation radicals of the ruthenium(II) porphyrin monocarbonyl complex and its derivatives incorporated into HRP afford unbroadened proton NMR spectra from which electron spin distributions on the porphyrin periphery, especially at the meso carbon, can be deduced, and thereby the symmetry of the π-cation radical orbital (a_{1u} and a_{2u}) is readily discerned. However, some of the NMR spectral features of this radical and its related compounds, especially their temperature, counteranion, and ligand effects remained open to further studies. In order to better understand the structural factors which affect the electronic structure of the metalloporphyrin π-cation radicals and to shed more light on the current dispute over assignment of their $^2A_{1u}$ and $^2A_{2u}$ electronic states in the model and hemoprotein compounds, we have performed here a comprehensive study of proton and deuterium NMR of ruthenium(II), Cobalt(III), and magnesium(II) porphyrin π-cation radicals.

Experimental Section

Materials. Ruthenium(II) carbonyloctaethylporphyrin (OEP·Ru^{II}·Co) was prepared by a variant of the method of Tsutsui, Ostfeld, and Hoffman.[23] Ruthenium(II) carbonyl-*meso*-d_4-octaethylporphyrin (*meso*-d_4-OEP·Ru^{II}·CO) was prepared by the same procedure with use of *meso*-d_4-octaethylporphyrin. *meso*-d_4-Octaethylporphyrin was prepared by sulfuric acid-d_2 exchange.[24] Cobalt(II) and magnesium(II) *meso*-d_4-octaethylporphyrin were also prepared by the literature methods.[18,25]

Oxidation of metalloporphyrins to π-cation radicals was performed by adding a stoichiometric amount of Br_2 to the CD_2Cl_2 solution of each metalloporphyrin.

Spectral Measurements. Optical absorption spectral measurements were made on a Hitachi 330 spectrophotometer. Low-temperature spectra were obtained by using a DN1704 variable-temperature liquid-nitrogen cryostat (Oxford Instruments) equipped with a digital temperature controller-DTC2 (Oxford Instruments).

Proton NMR spectra at 300 MHz and deuterium NMR spectra at 46.1 MHz were recorded with a Nicolet NT-300 spectrometer equipped with a 1280 computer system. Proton chemical shifts are referenced to Me_4Si, and downfield shifts are given a positive sign. The sample concentration for the proton and deuterium NMR measurements was 5–10 mM.

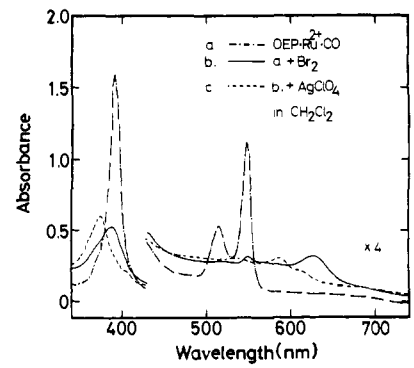

Figure 1. UV–vis spectra of OEP·Ru^{II}·CO (a), its one-electron-oxidized π-cation radical [OEP·Ru^{II}·CO]$^+$·Br^- (b), and [OEP·Ru^{II}·CO]$^+$·ClO_4^- (c) in CH_2Cl_2 at 23 °C.

Results

OEP·Ru^{II}·CO π-Cation Radicals. The CO complex of ruthenium(II) porphyrin electrochemically or chemically undergoes the ring oxidation to form a π-cation radical.[26,27] As was the case for carbonmonoxy ruthenium(II) mesoporphyrin IX dimethyl ester,[22] the octaethylporphyrin analogue forms a π-cation radical, [OEP·Ru^{II}·CO]$^+$·Br^- (**1**), by Br_2 oxidation in CH_2Cl_2 solution, and addition of perchlorate ion ($AgClO_4$) to this radical solution interchanges the counteranion to afford [OEP·Ru^{II}·CO]$^+$·ClO_4^- (**2**). Figure 1 shows the UV–vis absorption spectra of these two radical species. The spectrum of **1** has an intense absorption peak at 628 nm in the visible region, which resembles that of the $^2A_{1u}$ state porphyrin π-cation radicals of other metalloporphyrin complexes such as [OEP·Mg^{II}]$^+$· and [OEP·Zn^{II}]$^+$·,[28] while that of the perchlorate species was characteristic of the $^2A_{2u}$ state porphyrin π-cation radical such as [TMP·Zn^{II}]$^+$· and [TPP·Zn^{II}]$^+$·.[18] These porphyrin π-cations exhibited a typical ESR signal of a free radical at 77 K. Although the radical **2** gave a single-line ESR signal with $g = 2.000$ at room temperature, the ESR spectrum of **1** was beyond detection at this temperature due to too much broadening.

The proton NMR spectra of **1** and **2** at room temperature are illustrated in Figure 2A. The paramagnetically shifted proton peaks of **1** are surprisingly sharp and well-resolved, presumably due to a very short electron spin relaxation time. These proton resonances are readily assigned as follows: CH_3 of the ethyl group at 4.4 ppm, CH_2 at 24 and 30 ppm, and meso H at −35 ppm. The meso H assignment was confirmed by disappearance of this particular proton signal for the radical prepared from *meso*-d_4-OEP·Ru^{II}·CO. The radical **2** affords a substantially broadened CH_2 proton resonance in the downfield region and a broad meso proton signal at a shoulder of the CH_2 signal. Assignment of the meso H signal for **2** was further confirmed by the deuterium NMR measurement of the corresponding compound deuterated at the meso position.

It has been well established that deuterium NMR is often more suitable than proton NMR for the studies of the paramagnetic species[29,30] because the deuterium spectrum does not experience

(18) Fajer, J.; Borg, D. C.; Forman, A.; Dolphin, D.; Felton, R. H. *J. Am. Chem. Soc.* **1970**, *92*, 3451–3459.
(19) Maggiora, G. M. *J. Am. Chem. Soc.* **1973**, *95*, 6555–6559.
(20) Rutter, R.; Valentine, M.; Hendrich, M. P.; Hager, L. P.; Debrunner, P. G. *Biochemistry* **1983**, *22*, 4769–4774.
(21) Dinello, R. K.; Dolphin, D. *J. Biol. Chem.* **1981**, *256*, 6903–6912.
(22) Morishima, I.; Shiro, Y.; Takamuki, Y. *J. Am. Chem. Soc.* **1983**, *105*, 6168–6170.
(23) Tsutsui, M.; Ostfeld, D.; Hoffman, L. M. *J. Am. Chem. Soc.* **1971**, *93*, 1820–1823.
(24) Bonnett, R.; Gale, I. A. D.; Stephenson, G. F. *J. Chem. Soc. C* **1967**, 1168–1172.
(25) Furhop, J.-H.; Smith, K. M. In "Porphyrins and *Metalloporphyrins*": Smith, K. M., Ed.; Elsevier: Amsterdam, 1975; p 798.
(26) (a) Brown, G. M.; Hopf, F. R.; Fergusson, J. A.; Meyer, T. J.; Whitten, D. G. *J. Am. Chem. Soc.* **1973**, *95*, 5939–5942. (b) Brown, G. M.; Hopf, F. R.; Meyer, T. J.; Whitten, D. G. *Ibid.* **1975**, *97*, 5385–5390.
(27) Barley, M.; Becker, J. Y.; Domazetis, G.; Dolphin, D.; James, B. R. *J. Chem. Soc., Chem. Commun.* **1981**, 982–983; *Can. J. Chem.* **1983**, *61*, 2389–2396.
(28) Wolberg, A.; Manassen, J. *J. Am. Chem. Soc.* **1970**, *92*, 2982–2991.
(29) Shirazi, A.; Goff, H. M. *J. Am. Chem. Soc.* **1982**, *104*, 6318–6322.

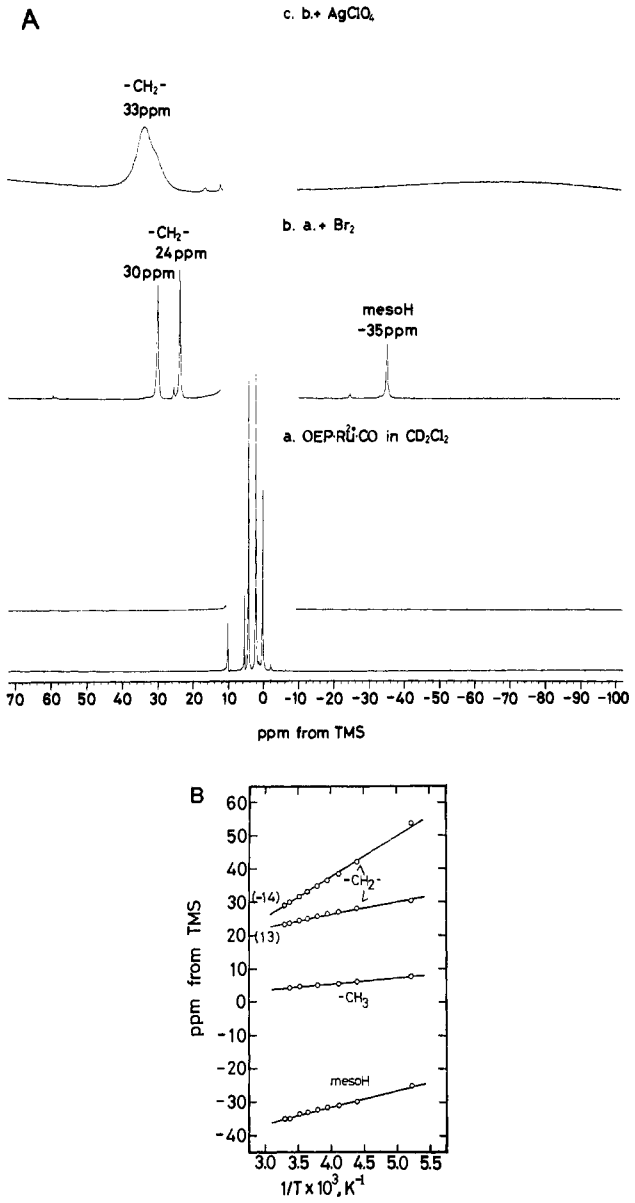

Figure 2. (A) Proton NMR spectra of OEP·Ru^{II}·CO (a), its one-electron-oxidized π-cation radical [OEP·Ru^{II}·CO]$^+$·Br$^-$ (b), and [OEP·Ru^{II}·CO]$^+$·ClO$_4^-$ (c) in CD_2Cl_2 at 23 °C. (B) Temperature dependence of the proton resonances of [OEP·Ru^{II}·CO]$^+$·Br$^-$. The chemical shifts are plotted against $1/T$ (Curie's plot). The apparent intercepts of methylene peaks at $1/T = 0$ are given in parentheses on the left.

unwanted broadening which is often encountered in the proton spectrum, like the ^{1}H spectrum of **2** in this study. Figure 3 shows D NMR spectra of *meso-d*$_4$-**1** and *meso-d*$_4$-**2**. The advantage of the use of D NMR is obviously seen for the porphyrin π-cation radical **2**.

An isotropic ^{1}H (or D) NMR hyperfine shift for the π-radical system is related through eq 1 and 2 to the π-electron spin density at the carbon to which the proton (or deuterium) is attached.

$$(\Delta H/H)_{iso} = A^H(\gamma_e/\gamma_H)[g\beta S(S+1)/3kT] \quad (1)$$

$$A^H = Q\rho_c \quad (2)$$

Here eq 1 relates the observed isotropic shift $(\Delta H/H)_{iso}$ with the hyperfine coupling constant of the proton (A^H) (downfield proton shifts correspond to a positive value of A^H).[31] Equation 2 is the

(30) Wheeler, W. D.; Kaizaki, S.; Legg, J. I. *Inorg. Chem.* **1982**, *21*, 3248–3250.

(31) (a) Jesson, J. P. "NMR of Paramagnetic Molecules"; La Mar, G. N., Horrocks, W. D., Holm, R. H., Eds.; Academic Press: New York, 1973; pp 1–52. (b) Kreilick, R. W., ref 31a, pp 595–626.

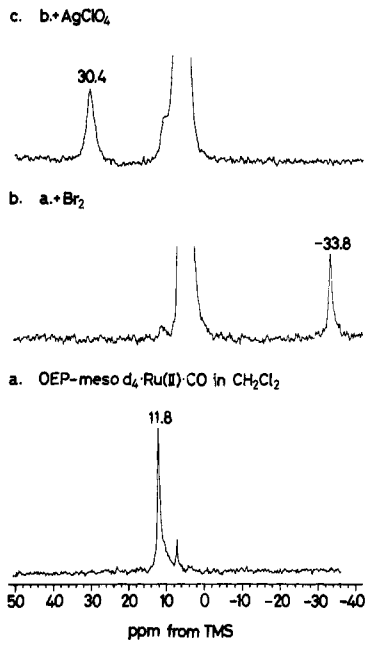

Figure 3. Deuterium NMR spectra of *meso-d*$_4$-OEP·Ru^{II}·CO (a), its one-electron-oxidized π-cation radical [*meso-d*$_4$-OEP·Ru^{II}·CO]$^+$·Br$^-$ (b), and [*meso-d*$_4$-OEP·Ru^{II}·CO]$^+$·ClO$_4^-$ (c) in CH_2Cl_2 at 23 °C.

Table I. Meso Deuterium Isotropic Shifts $(\Delta H/H)_{iso}$ and Spin Densities on the Meso Carbon (ρ_c) for OEP·Ru^{II}·CO π-Cation Radicals

	experiment[a] [OEP·Ru^{II}]$^+$·X		theory[b]	
	X = Br$^-$	X = ClO$_4^-$	$^2A_{1u}$	$^2A_{2u}$
$(\Delta H/H)_{iso}$, ppm	−44	+20	−2	−322
ρ_c	0.026	−0.012	0.0012	0.1932

[a] Spin densities are obtained through eq 1 and 2, T = 296 K. [b] The values are obtained from ref 18, and isotropic shifts are calculated through eq 1 and 2, T = 296 K.

McConnel relation[32] which connects A^H with the π spin density on the carbon (ρ_c). With these equations, the observed hyperfine shifts of the meso H (or D) are translated into π spin density at the meso carbon for **1** and **2** which are compiled in Table I together with the MO-calculated values for a metal-free porphyrin π-cation radical.

The temperature dependence of the hyperfine-shifted proton resonances of **1** is illustrated in Figure 2B in the form of the Curie plot. Inspection of the figure shows that the unusual non-Curie law behavior is seen for the meso proton resonance. The methylene proton resonances which have intercepts of −14 and 13 ppm at $1/T = 0$, beyond the diamagnetic shift region, do not appear to follow the normal Curie law behavior. Similar non-Curie law behavior was also found for the meso D signal of **2**; temperature dependence of the meso D resonance was extrapolated to $1/T = 0$, with an intercept of −12 ppm. These unusual temperature dependences could not be accounted for if **1** and **2** are in a single spin state.

To gain further insight into this temperature-dependent behavior, the absorption spectrum of **1** was studied at various temperatures from 193 to 290 K. Figure 4 shows that as the temperature raises, the peak at 622 nm is red shifted with an isosbestic point at 626 nm. This spectral change was fully reversible with raising or lowering temperature. The absorption spectrum of **2** also exhibited temperature dependence with an isosbestic point at 596 nm. The above variable-temperature NMR and absorption spectral studies clearly indicate that the π-cation radicals examined here are in a thermal equilibrium between two different electronic states, probably $^2A_{1u}$ and $^2A_{2u}$ states, which will be argued in detail in the Discussion section.

Since the highest filled π orbitals (a_{1u} or a_{2u}) of metalloporphyrin are nearly degenerate, the electronic ground state of

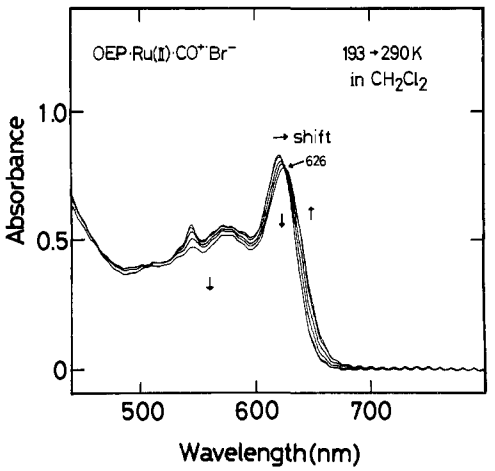

Figure 4. Visible absorption spectra of $[OEP{\cdot}Ru^{II}{\cdot}CO]^{+}{\cdot}Br^{-}$ 0.7 mM in the 193–290 K range (CH_2Cl_2 solvent). Temperature rises as indicated by the arrows.

its π-cation radical could be readily modulated by an axial ligand.[13] In order to study the effect of axial ligation on the electronic structure of porphyrin π-cation radical, we examined the proton and deuterium NMR spectrum of the imidazole complex of $[OEP{\cdot}Ru^{II}{\cdot}CO]^{+}Br^{-}$ and its meso-deuterated analogue, with much attention to the meso D hyperfine shifts. Since the radical was reducible to the neutral species in the presence of imidazole at room temperature, the titration of imidazole to the radical solution was performed at −45 °C. At this temperature, the meso deuterium signal of the imidazole-free radical is observed at −28.6 ppm (Figure 5A (a)). With addition of imidazole, a new meso deuterium signal grows up at 11.4 ppm, with concomitant decrease in intensity of the signal for the ligand-free species. Formation of the monoimidazole–porphyrin π-cation radical complexes, $[OEP{\cdot}Ru^{II}(CO)(Im)]^{+}{\cdot}Br^{-}$ (**3**), was completed with a stoichiometric amount of imiazole as shown in Figure 5A, b and c. These spectral changes indicate that the ligand exchange between liganded and non-liganded radicals is slow on the NMR time scale. The formation of the monoimidazole complex was also confirmed by observing the deuterium resonances of the Ru(II)-bound imidazole-d_4 at +13 to +16 ppm in the downfield paramagnetic region. The monoimidazole complex of this radical also afforded a relatively sharp proton NMR spectrum, in which the methylene ^1H shift exhibited downfield bias by 3 ppm upon imidazole complex formation (Figure 5B).

OEP·Co^{III} π-Cation Radicals. It has been reported that a stable π-cation radical $[OEP{\cdot}CO^{III}]^{2+}{\cdot}2X^{-}$, which is produced by two-electron oxidation of cobaltous octaethylporphyrin, $OEP{\cdot}CO^{II}$, exhibits $^2A_{1u}$ and $^2A_{2u}$ optical spectra interchangeably as a function of the counteranion, $X^{-} = Br^{-}$ (**4**) or ClO_4^{-} (**5**).[6a] We reexamined the electronic states of these porphyrin π-cation radicals by proton NMR (Figure 6A). The proton spectrum of **5** was beyond detection due to too much broadening. Therefore, we also studied the deuterium NMR for meso-deuterated compounds (Figure 6B). The meso deuterium resonance of $OEP{\cdot}CO^{II}$ in chloroform (Figure 6B a) was detected at 30.0 ppm due to a metal-centered paramagnetism (Co^{II}, d_7, $S = {}^1/_2$). Figure 6B, b and c, shows the D NMR spectra of its two-electron-oxidized radicals, **4** and **5**. Since the metal center is in a diamagnetic state (Co^{III}, d_6, $S = 0$), the hyperfine shift of the meso deuterium for these radicals originates from a porphyrin-centered paramagnetism. It is noteworthy that the meso deuterium peak for **4** is observed in the upfield region (−67.8 ppm), while that for **5** is observed in the downfield region (22.6 ppm). These radicals also exhibited non-Curie law behavior of the temperature dependence of the meso D resonance shift (Figure 7), which also could be interpreted in terms of the thermal equilibrium between $^2A_{1u}$ and $^2A_{2u}$ states, as is the case for ruthenium(II) porphyrin radicals **1** and **2**.

OEP·Mg^{II} π-Cation Radicals. We have also studied the deuterium NMR spectrum of *meso*-d_4-$OEP{\cdot}Mg^{II+}{\cdot}ClO_4^{-}$ (**6**) in methylene chloride and methanol solutions. It was previously

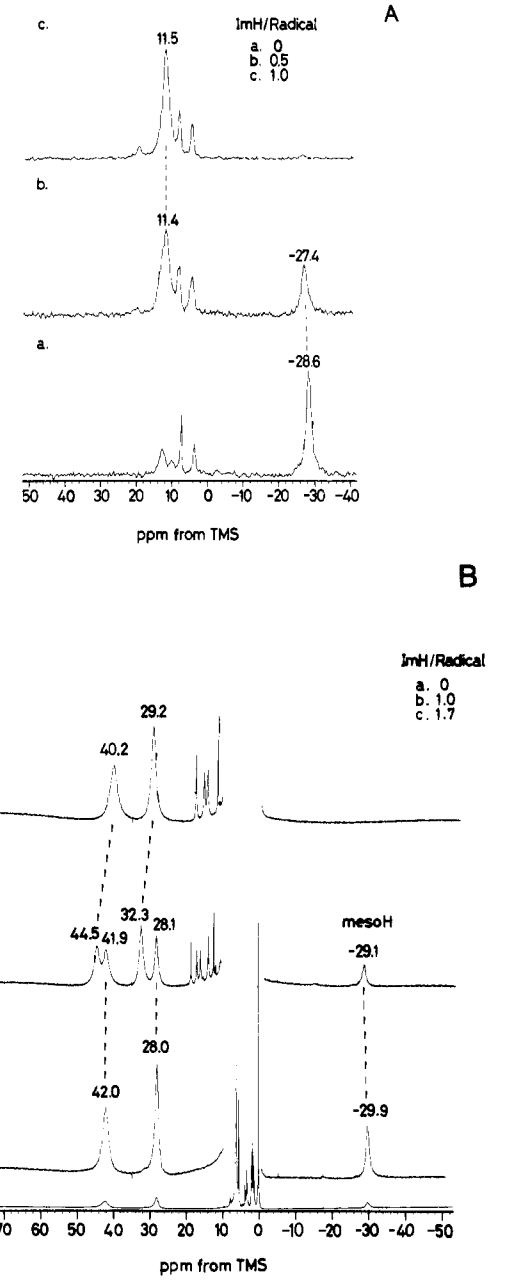

Figure 5. (A) Deuterium NMR spectra for the titration of $[meso\text{-}d_4\text{-}OEP{\cdot}Ru^{II}{\cdot}CO]^{+}{\cdot}Br^{-}$ with imidazole in CH_2Cl_2 at −45 °C. Imidazole added: (a) 0.0 equiv, (b) 0.5 equiv, (c) 1.0 equiv. (B) Proton NMR spectra for the titration of $[OEP{\cdot}Ru^{II}{\cdot}CO]^{+}{\cdot}Br^{-}$ with imidazole in CH_2Cl_2 at −45 °C.

reported that this radical forms a diamagnetic dimer at low temperatures.[18] In agreement with this result, **6** in methylene chloride at −50 °C afforded a sharp meso D resonance at 6 ppm in the diamagnetic region. With a rise in temperature to 23 °C, the meso deuterium signal shifted upfield to −1.3 ppm, accompanied by significant broadening. This signal broadening could be due to the monomer radical, in which the meso D signal is supposed to be extremely broadened. This observation suggests that the exchange between the monomeric radical and the diamagnetic dimer is very fast on the NMR time scale.

We then tried to estimate the limiting shift of meso D for the monomeric radical **6**. The dimer of $OEP{\cdot}Mg^{II}$ π-cation radical exhibits an absorption spectrum at 950 nm.[18] Since the extinction coefficient[18] of this absorption and the total concentration of the porphyrin radical are known, the concentrations of both the monomer and the dimer can be determined at various temperatures. From the analysis of this monomer–dimer equilibrium by optical spectra using a 1-mm optical cell, about 70% of the radical

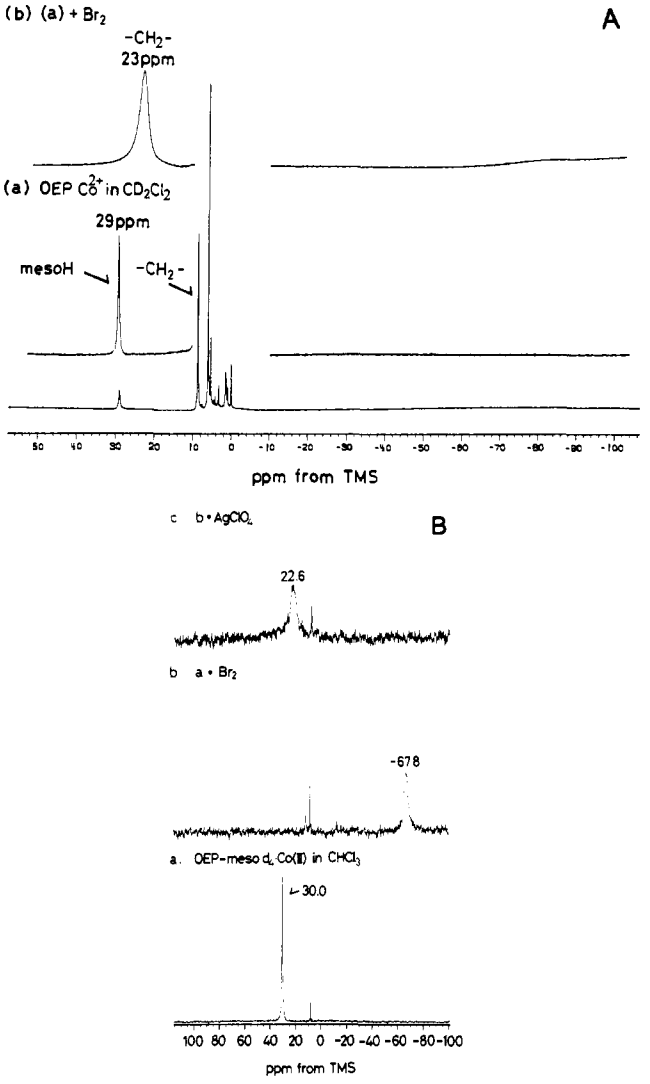

Figure 6. (A) Proton NMR spectra of OEP·Co^{II} (a) and its two-electron-oxidized species $[OEP{\cdot}Co^{III}]^{2+}2Br^-$ (b). (B) Deuterium NMR spectra of *meso*-d_4-OEP·Co^{II} (a), its two-electron-oxidized π-cation radical $[meso\text{-}d_4\text{-}OEP{\cdot}Co^{III}]^{2+}{\cdot}2Br^-$ (b), and $[meso\text{-}d_4\text{-}OEP{\cdot}Co^{III}]^{2+}{\cdot}2ClO_4^-$ (c) in $CHCl_3$ at 23 °C.

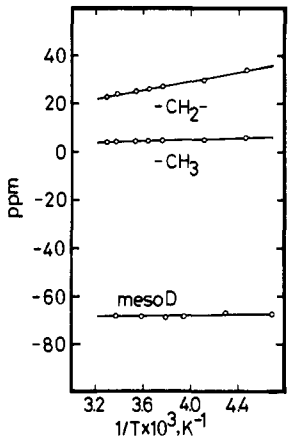

Figure 7. Curie's plot for $[OEP{\cdot}Co^{III}]^{2+}{\cdot}2Br^-$.

is monomeric at the temperature and concentration examined for the NMR measurements. Although quantitative estimation of the limiting shift of the meso D for the monomeric radical **6** was not successful, the hyperfine shifted resonance of the meso proton is supposed to be in the upfield region.

We have also examined the deuterium NMR of **6** in CH_3OH solution to compare with the ESR results.[18] At −80 °C, a single broad resonance was observed in the downfield region from 0 to

Scheme I

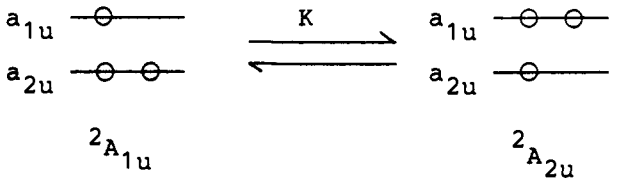

10 ppm, which is considered to correspond to a diamagnetic dimer, as inferred from UV spectral measurements. With raising temperature to −20 °C, this signal gradually decreased in intensity and no signal was observed in the paramagnetic shift region. This spectral feature for **6** in CH_3OH is quite different from that for **6** in CH_2Cl_2. The electronic structure of **6** in CH_3OH appears quite different from that of **6** in CH_2Cl_2, in agreement with the ESR result that the hyperfine coupling is observed only for the former system.[13,18]

Discussion

Electronic State of Metalloporphyrin π-Cation Radicals. A radical center is normally expected to exhibit an ESR spectrum and to induce extreme broadening of NMR resonances. Recently, however, Goff et al.[33] reported that the iron(III) porphyrin π-cation radicals, which were generated by electrochemical and selected chemical methods, exhibited well-defined NMR spectra, and they suggested that the π-electron spin in the proximity of the paramagnetic iron atom should promote electron spin relaxation to yield NMR signals which are not excessively broadened. But in the case of carbon monoxy ruthenium(II) porphyrin π-cation radical where the metal center is diamagnetic (Ru^{II}, d_6, $S = 0$), unusually sharp resonances in its ^1H NMR spectra should demand enhanced electron spin relaxation mechanisms other than that for the iron(III) porphyrin π-cation radicals.[22] Quite a normal value of $g = 2.00$ at 77 K for the octaethylporphyrin ruthenium(II) π-cation radicals may allow us to expect that a spin–orbit coupling at the metal atom may not be responsible for enhanced electron spin relaxation. Coupling of metal and π-orbitals or counteranion and π-radical could cause the short electron spin relaxation.[6a] More probably, mixing of degenerate or nearly degenerate radicals ($^2A_{1u}$ and $^2A_{2u}$) may also induce enhanced electron spin relaxation by electron exchange between these two radical states. The present finding of the unusual non-Curie law behavior of the hyperfine-shifted proton resonances and the temperature-dependent features of the electronic absorption spectra for OEP·Ru^{II}·CO π-cation radicals could be explained by assuming that this radical is in a thermal equilibrium between two different electronic states, $^2A_{1u}$ and $^2A_{2u}$. In other words two distinct states are thermally populated for the π-cation radical and the mixing is modulated by temperature.

The salient features of $^2A_{2u}$ porphyrin π-cation radical are distribution of a substantial amount of positive spin density at the meso carbons and the pyrrole nitrogens, while the radical orbital in $^2A_{1u}$ cations has a node at these atoms (D_{4h} symmetry).[18] Since the isotropic shift of the meso proton is proportional to the meso carbon spin density (eq 1 and 2), the typical $^2A_{2u}$ radical is expected to induce a large upfield contact shift for the meso proton and the $^2A_{1u}$ radical exhibits a downfield bias. If we assume that the a_{1u} orbital possesses slightly higher energy than the a_{2u} orbital, the thermal mixing of the $^2A_{2u}$ state increases with increasing temperature (Scheme I) to afford more positive spin density at the meso position, eventually inducing more upfield isotropic shift, as is shown in Figure 2B.

The porphyrin π-cation radical with predominant $^2A_{2u}$ state has been well characterized by the ESR studies of various meso-tetraalkyl or tetraphenyl metalloporphyrin π-cation radicals which exhibit substantially large hyperfine coupling constants for the pyrrole nitrogen and the proton of the meso substituents.[6c,e] Contrary to this, the porphyrin π-cation radical which is pre-

(32) McConnell, H. M. *J. Chem. Phys.* **1956**, *24*, 764.
(33) Phillippi, M. A.; Goff, H. M. *J. Am. Chem. Soc.* **1982**, *104*, 6026–6034.

Table II. Thermodynamic Values for the $^2A_{1u} \rightleftharpoons {}^2H_{2u}$ Equilibrium of Some Metalloporphyrin π-Cation Radicals (at 296 K)[a]

π-cation radicals	choice of the limiting shift[a]	α, %	ΔH, cal/mol	ΔS, eu
$[OEP{\cdot}Ru^{II}{\cdot}CO]^+{\cdot}Br^-$ (**1**)	1	57.1	−299	−0.205
	2	73.5	−504	+0.174
$[OEP{\cdot}Ru^{II}{\cdot}CO]^+{\cdot}ClO_4^-$ (**2**)	1	75.0	−139	+0.873
	2	96.6	−1460	+0.904
$[OEP{\cdot}Ru^{II}{\cdot}CO{\cdot}Im]^+{\cdot}Br^-$ (**3**)[b]	1	69.8	−92	+0.635
$[OEP{\cdot}Co^{III}]^{2+}{\cdot}2Br^-$ (**4**)	1	48.1	−390	−0.731
$[OEP{\cdot}Co^{III}]^{2+}{\cdot}2ClO_4^-$ (**5**)	1	72.9	−11	+0.972

[a] The set 1 for δ^2A_{1u} = +111 ppm and δ^2A_{2u} = −252 ppm at 296 K. The set 2 for δ^2A_{1u} = +30 ppm and δ^2A_{2u} = −252 ppm at 296 K. [b] At 228 K.

dominantly in $^2A_{1u}$ state is quite limited.[18,28] $[OEP{\cdot}Mg^{II}]^+{\cdot}ClO_4^-$ has been assigned as a $^2A_{1u}$ π-cation with an ESR coupling constant of A^H = 1.48 G for the meso proton in methanol at −50 °C.[18] This coupling constant is translated into π spin density $\rho_c = \pm 0.066$ at the meso carbon. Since an a_{1u} orbital has a node at the meso carbon, a negative spin density due to electron correlation effect is expected at the meso position. In fact, the downfield contact shift for the meso proton which corresponds to the negative π spin density on the carbon is induced in $[OEP{\cdot}Ru^{II}{\cdot}CO]^+{\cdot}ClO_4^-$. In this sense, negative spin density of $\rho_c = -0.066$ at the meso carbon in $[OEP{\cdot}Mg^{II}]^+{\cdot}ClO_4^-$ appears more favorable. The small upfield contact shift for the meso H in $[OEP{\cdot}Ru^{II}{\cdot}CO]^+{\cdot}Br^-$ could, therefore, be reasonably accounted for if we assume that the $^2A_{2u}$ state is mixed to the predominant $^2A_{1u}$ state. We then tried to determine quantitatively the thermodynamic parameters of this thermal equilibrium (equilibrium constant K) by using relation 3. The observed isotropic shift of

$$K = {}^2A_{1u}/{}^2A_{2u} = \alpha/(1-\alpha) \quad (3)$$

$$\delta_{obsd} = \alpha\delta^2A_{1u} + (1-\alpha)\delta^2A_{2u} \quad (4)$$

the meso proton can be expressed as eq 4, where δ^2A_{1u} and δ^2A_{2u} are the limiting shifts for corresponding typical states and α is the content propotion of the $^2A_{1u}$ state. The experimental value of δ^2A_{2u} (−252 ppm at 296 K) can be obtained through eq 1 from a meso methyl proton ESR coupling constant, A^{CH_3} = 5.90 G, measured for $[TMP{\cdot}Zn^{II}]^+{\cdot}ClO_4^-$, a typical $^2A_{2u}$ state porphyrin π-cation radical.[6e] The δ^2A_{1u} value (+110 ppm at 296 K) also can be estimated from A^H = 1.48 G for $[OEP{\cdot}Mg^{II}]^+{\cdot}ClO_4^-$ in methanol.[18] With these limiting shifts and observed shifts for the meso proton at various temperatures, the equilibrium constant K was obtained at each temperature. Plots of log K vs. $1/T$ gave a straight line from which ΔH = −299 cal/mol and ΔS = −0.205 eu are obtained for $[OEP{\cdot}Ru^{II}{\cdot}CO]^+{\cdot}Br^-$ and ΔH = −139 cal/mol and ΔS = −0.205 eu were obtained for $[OEP{\cdot}Ru^{II}{\cdot}CO]^+{\cdot}ClO_4^-$. A similar analysis was also performed for π-cation radicals **3**, **4**, and **5**, and the results are compiled in Table II. Choice of the δ^2A_{1u} value in the range from +30 to +80 ppm did not lead to a major change in the above results.

Thermal spin equilibrium between the high- and low-spin states of the heme iron has been shown to be a unique property of hemoprotein. Neya and Morishima[34] reported that the 6-coordinate complex, hemin-N_3^--$(CH_3)_2SO$, was in a thermal spin equiibrium and made a similar analysis to obtain its thermodynamic parameters ΔH = −136 cal/mol and ΔS = −0.975 eu. These thermodynamic parameters are comparable to the present results. This implies that the thermal mixing of two electronic states, $^2A_{1u}$ and $^2A_{2u}$, could readily be caused as is the case for thermal spin admixture when they are energetically close to each other.

Each π-cation radical in the $^2A_{1u}$ or $^2A_{2u}$ state exhibits the characteristic visible absorption spectrum respectively. The visible spectrum of $[OEP{\cdot}Mg^{II}]^+{\cdot}$, which has been assigned to the $^2A_{1u}$ state, is characterized by a major absorption peak near 700 nm with a high energy shoulder, while that of $[TPP{\cdot}Zn^{II}]^+{\cdot}$ ($^2A_{2u}$) shows a broad and featureless absorption band in the region 500–700 nm. On the basis of these results, the electronic spectrum of **1**, $[OEP{\cdot}Ru^{II}{\cdot}CO]^+{\cdot}Br^-$, has been assigned to the $^2A_{1u}$ state and that of **2**, $[OEP{\cdot}Ru^{II}{\cdot}CO]^+{\cdot}ClO_4^-$, to the $^2A_{2u}$ state. The present NMR results, however, show that **1** senses negative spin density at the meso proton (positive spin density at meso carbon), while spin density with an opposite sign is induced for **2**, indicating the latter is more $^2A_{1u}$ like than the former. The upfield bias of the meso proton signal for **1** compared to **2** could be due to this cause. The downfield bias of the CH_2 proton contact shift for **2** compared with **1** also supports this view, since MO-calculated spin density on the pyrrole β carbon is larger for the $^2A_{1u}$ state than for the $^2A_{2u}$ state.[6h] This is strongly in disagreement with the well-documented assignment from the electronic spectra.

The deuterium NMR results of cobaltic porphyrin π-cation radicals also show that the perchlorate species (**5**) is more $^2A_{1u}$ like than the bromide species (**4**) (Table II), in disagreement with the assignment by the electronic spectra. The ^{59}Co ($I = {}^7/_2$) ESR coupling constant (A^{Co} = 1.2 G) has been observed for **5**, while it has not been detected for **4**.[6a] Observation of the metal coupling in the ESR spectrum of metalloporphyrin π-cation radicals indicates that spin density resides on the central metal orbital, characteristic of the $^2A_{2u}$ state. Since $[TPP{\cdot}Co^{III}]^{2+}{\cdot}2ClO_4^-$ is predominantly in the $^2A_{2u}$ state with a large metal coupling constant (A^{Co} = 5.7 G),[28] the coupling constant A^{Co} = 1.2 G for $[OEP{\cdot}Co^{III}]^{2+}{\cdot}2ClO_4^-$ could be reasonably explained if 20% of the $^2A_{2u}$ state is mixed to the $^2A_{1u}$ state. This is in agreement with the suggestion from the present study of the meso deuterium NMR shift (Table II). Accordingly, the observation of the metal coupling constant is not necessarily a diagnosis of the $^2A_{2u}$ state of the metalloporphyrin π-cation radical.

The present results on the meso deuterium NMR and the visible absorption spectroscopic analysis of $[OEP{\cdot}Mg^{II}]^+{\cdot}ClO_4^-$ in CH_2Cl_2, which exhibits a $^2A_{1u}$ type spectrum, indicate that the meso deuterium signal of the monomer of this radical would exist in the upfield region, characteristic of the $^2A_{2u}$ π-cation radical. It is therefore likely that in the magnesium(II) porphyrin π-cation radical in CH_2Cl_2 solution the $^2A_{1u}$ state is mixed to some extent with the $^2A_{2u}$ state and not in the predominant $^2A_{1u}$ state.

Electronic State of HRP Compound I. Previously we reported the proton NMR spectrum of ruthenium(II) mesoporphyrin π-cation radical incorporated into HRP,[22] and from the close resemblance between this spectrum and that of HRP compound I, we suggested that large hyperfine shifts of the heme peripheral protons in HRP compound I might result mostly from the π-cation radical center rather than from the paramagnetic metal center. It then follows from this spectral similarity that ruthenium(II) octaethylporphyrin π-cation radical, which is a model compound of $HRP{\cdot}Ru^{II}{\cdot}CO$ π-cation radical, could help us to examine the electronic structures of the π-cation radical center in HRP compound I.

As described in the above section, the visible absorption spectrum does not serve as a diagnosis for characterization of the electronic structure of the π-cation radical. The present finding that coordination of imidazole to $[OEP{\cdot}Ru^{II}{\cdot}CO]^+{\cdot}Br^-$ induced a downfield bias of the hyperfine shifts for the meso deuterium signal and methylene proton signals as well suggests that the binding of the axial ligand to this radical more favors $^2A_{1u}$ state in its electronic ground state. Quite a small magnitude (~15 ppm) of deuterium hyperfine shifts for the Ru(II)-bound imidazole-d_4 also supports this view, since $^2A_{1u}$ π-cation places a small amount

(34) Neya, S.; Morishima, I. *J. Am. Chem. Soc.* **1982**, *104*, 5658–5661.

of spin density on the metal and eventually on the axial ligand.[6h] This may allow us to suggest that the electronic state of HRP compound I is more $^2A_{1u}$ like rather than $^2A_{2u}$, which has long been accepted on the basis of electronic absorption spectra and ENDOR results. ENDOR results of HRP compound I,[12] however, could be reasonably explained by assuming this compound to be in the $^2A_{1u}$ state, since the experimentally estimated average spin densities distributed on porphyrin nitrogen and carbon are very close to MO theoretical values calculated for an $^2A_{1u}$ radical.[7] Moreover, the meso proton coupling by the ENDOR experiment appears closer to the MO results for the $^2A_{1u}$ state if we assume that A^H has a negative sign. By analogy with the present studies on the porphyrin π-cation radical, the electronic state of the porphyrin π-cation of HRP compound I is likely formulated as $^2A_{1u}$ mixed to some extent with $^2A_{2u}$. This review has also been suggested by Stillman et al.[35] on the basis of their MCD results that there is no distinct difference in the MCD spectra of CAT and HRP compounds I, both of which do not resemble either of the MCD spectrum for typical $^2A_{1u}$ or $^2A_{2u}$ porphyrin π-cation radical. At any event, deuterium NMR examination of HRP compound I reconstituted with the meso deuterated protohemin could directly test our present speculation on the electronic state of this radical center, which is planned in our laboratory.

Keeping in mind the above discussion, we would like to make some comment on the NMR spectral features of HRP compound I. It was proposed that weak coupling between electron spins on iron(IV) and on the porphyrin radical results in enhanced electron spin relaxation, eventually leading to the sharp NMR and very broadened ESR spectra of HRP compound I.[8,36] However, the possibility of the enhanced electron spin relaxation caused by fast exchange between $^2A_{1u}$ and $^2A_{2u}$ porphyrin radical states should also be taken into account to explain the unique spectral features of NMR and ESR spectra of HRP compound I. This mixing mechanism could also be responsible for ambiguities in assigning their optical spectra to either $^2A_{1u}$ or $^2A_{2u}$ type. The subtle structural changes in the heme environments of HRP and CAT could modulate the mixing of two electronic states. Details of the studies of the π-cation radicals of ruthenium(II) meso and deuteroporphyrin monocarbonyl complexes and their derivatives incorporated into HRP will be published elsewhere.

Acknowledgment. The authors thank Drs. T. Kawamura and H. Ohya-Nishiguchi for helpful discussions. This work is supported by a grant from the Ministry of Education, Japan (57470119).

(35) Browett, W. R.; Stillman, M. J. *Biochim. Biophys. Acta* **1981**, *660*, 1-7. (b) Browrett, W. R.; Stillman, M. J. *Inorg. Chim. Acta* **1981**, *49*, 69-77.

(36) Morishima, I.; Ogawa, S. *J. Am. Chem. Soc.* **1978**, *100*, 7125-7128. (b) Morishima, I.; Ogawa, S. *Biochemistry* **1978**, 4384-4388. 4384-4388. (c) Morishima, I.; Ogawa, S. *Biochem. Biophys. Res. Commun.* **1978**, *83*, 946-953.

Low-Temperature ^{13}C Magnetic Resonance in Solids. 3. Linear and Pseudolinear Molecules

Alvin J. Beeler,[1] Anita M. Orendt, David M. Grant,* Peter W. Cutts, Josef Michl,* Kurt W. Zilm, John W. Downing, Julio C. Facelli, Michael S. Schindler,[2] and Werner Kutzelnigg[2]

Contribution from the Department of Chemistry, University of Utah, Salt Lake City, Utah 84112. *Received June 4, 1984*

Abstract: The solid-state low-temperature ^{13}C NMR spectra of five linear (CO, CO_2, OCS, C_3O_2, acetylene) and four pseudolinear (propyne, 2-butyne, allene, ketene) molecules have been obtained. The assignments of the shielding tensor axes are made from symmetry in all but allene and ketene. In these pseudolinear molecules shift assignments are based on ab initio calculations by the IGLO version of the coupled Hartree–Fock method. Except for carbon monoxide, the parallel component of the chemical shift tensor ($\sigma_\parallel$) for C_∞ is remarkably constant at -90 ppm from Me_4Si, establishing a reference point for discussing the paramagnetic shielding terms. Variations in both the diamagnetic term and off-center shielding terms of both varieties were found to be relatively small. Destruction of the C_∞ symmetry in molecules having hydrogen lying off the C–C axis of pseudolinear molecules resulted in major shifts in the tensorial shieldings. Theoretical correlation of the relative experimental shielding values is very good although the agreement of magnitudes in the low-field range worsens as one moves away from the methane shift which is used as a fiducial value to establish the comparison. It is concluded that the theory faithfully represents the shielding phenomena and may be used to assign shielding components to specific spatial orientations when symmetry features or other unequivocal information is lacking.

Recent NMR work[3-8] on small molecules at low temperatures has resulted from the pioneering work on cross polarization (CP) by Hartman and Hahn[9] and Pines, Gibby, and Waugh.[10] While the initial low-temperature work with ^{13}C CP experiments was conducted at liquid nitrogen temperatures, others[7,11] have extended the method to much lower temperatures using matrix isolation techniques developed earlier in optical and electron spin resonance spectroscopy.[12] Matrix isolation techniques in NMR have also benefited from the use of labeled compounds to enhance the signal-to-noise ratio and to provide information on the ^{13}C–^{13}C dipolar interaction. Isolation and immobilization of both reactive

(1) Present address: E. I. du Pont de Nemours & Co., Richmond, VA.
(2) Ruhr Universitat Bochum, Germany.
(3) Linder, J.; Hohener, A.; Ernst, R. R. *J. Magn. Reson.* **1979**, *35*, 379.
(4) Kohl, J. E.; Semack, M. G.; White D. *J. Chem. Phys.* **1978**, *69*, 5378.
(5) Pines, A.; Gibby, M. G.; Waugh, J. S. *J. Chem. Phys.* **1973**, *59*, 569.
(6) Gibson, A. A. V.; Scott, T. A.; Fukushima, E. *J. Magn. Reson.* **1977**, *27*, 29.
(7) Zilm, K. W.; Conlin, R. T.; Grant, D. M.; Michl, J. *J. Am. Chem. Soc.* **1980**, *100*, 6672.
(8) Ishol, L. M.; Scott, T. A. *J. Magn. Reson.* **1977**, *27*, 23.
(9) Hartman, S. R.; Hahn, E. L. *Phys. Rev.* **1962**, *128*, 2042.
(10) Pines, A.; Gibby, M. G.; Waugh, J. S. *Chem. Phys. Lett.* **1972**, *15*, 373.
(11) Zilm, K. W.; Grant, D. M. *J. Am. Chem. Soc.* **1981**, *103*, 2913.
(12) Moskovits, M., Ozin, G. A., Eds. "Cryochemistry"; John Wiley and Sons, Inc.: New York, 1976.

0002-7863/84/1506-7672$01.50/0